J Bio Tribo Corros (2017) 3:10
DOI 10.1007/s40735-016-0070-z

Controlling the Rate of Dissolution of Mild Steel in Sulfuric Acid Through the Adsorption and Inhibition Characteristics of (4-(4-Hydroxybenzylideneamino)-4H-1,2,4-Triazole-3,5-diyl) dimethanol (HATD)

M. Prajila[1] · **Abraham Joseph**[1]

Received: 6 July 2016 / Revised: 22 December 2016 / Accepted: 24 December 2016 / Published online: 3 January 2017

Abstract Inhibition of mild steel corrosion in H_2SO_4 using a Schiff's base derived from 1,2,4-triazole, (4-(4-hydroxybenzylideneamino)-4H-1,2,4-triazole-3,5-diyl) dimethanol, has been investigated by weight loss, electrochemical, surface morphological, adsorption, and quantum chemical studies. It is found that inhibition efficiency increases with concentration of inhibitor and decreases with temperature. Results of polarization studies revealed the mixed type behavior of the inhibitor. Adsorption phenomenon follows Langmuir isotherm model, and values of free energy changes indicate that the mechanism involves both physisorption and chemisorption. Values of activation parameters revealed the endothermic nature of the corrosion process. Surface morphological studies support the prediction of the protection of metal by the formation of a surface film in the presence of the inhibitor. Geometry optimization of the inhibitor molecule is done by quantum chemical studies.

Keywords Mild steel · Acid corrosion · Inhibitor · Electrochemical studies

1 Introduction

One of the most serious problems the modern society facing is the corrosion of metals used in different fields. A wide range of industries affected by corrosion include oil production, oil refining, chemical and petrochemical manufacture, fertilizer production, power stations, and civil engineering structures involving buildings and bridges [1].The study of corrosion of mild steel in acid media has become important since sulfuric acid and hydrochloric acid are the medium generally used for industrial cleaning and acid descaling [2, 3].Corrosion process can be significantly suppressed by the incorporation of certain substances into the environment, which act as inhibitors. Organic compounds, particularly those containing heterocyclic rings, polar functional groups with N, O, and/or S atoms, received extensive application in this regard [4–11]. The inhibitors act at the interface between the metal and aqueous aggressive solution, and their interaction with the corroding metal surface via adsorption may either modify the mechanism of charge transfer reaction at the interface or reduce the surface area available for anodic and cathodic reactions [12].

Among various heterocyclic nitrogen-containing organic compounds, 1,2,4-triazole and its derivatives constitute one of the most biologically active classes of compounds having a wide spectrum of activities such as industrial, agro-chemical, and pharmaceutical applications [13–17]. In addition, substituted triazoles, particularly Schiff's bases, have been recently studied in considerable detail as effective corrosion inhibitors for mild steel in acid media [18–20]. Besides corrosion inhibitors, Schiff's bases are used as dyes, pigments, and catalysts for the activation of small molecules and other biological activities [21–25]. Structurally, a Schiff's base is a nitrogen analogue of an aldehyde or ketone, in which the carbonyl group (C=O) has been replaced by an imine (azomethine) group. They are considered as good corrosion inhibitors due to the presence of the [–C=N–] group, electron cloud on the aromatic ring, the electronegative nitrogen, and the oxygen/sulfur atoms in the molecule [26–28].The activity of Schiff's base molecules on metal surface is by the formation of thin and

✉ Abraham Joseph
drabrahamj@gmail.com

[1] Department of Chemistry, University of Calicut, Calicut University P O, Calicut, Kerala 673635, India

persistent adsorbed film, which decreases the metal corrosion by slowing down the anodic/cathodic reaction or both [29].Due to the importance of corrosion prevention, it is intended to study the inhibition behavior of a 1,2,4-triazole Schiff's base having biological significance. Therefore, the objective of the present study is to synthesize and investigate the corrosion inhibition behavior of 1,2,4-triazole-based Schiff's base (4-(4-hydroxybenzylideneamino)-4H-1,2,4-triazole-3,5-diyl)dimethanol (HATD) for mild steel in H_2SO_4 at three different temperatures. The effect of inhibitor concentration, acid concentration, and temperature on inhibition efficiency has also been monitored.

2 Experimental

2.1 Materials

The mild steel sample had the following composition (at.%): C (0.2%), Mn (1%), P (0.03%), S (0.02%), and Fe (98.75%). For electrochemical studies, mild steel coupons of 1 cm^2 area were exposed in each test. The samples were polished using different grades of emery papers and degreased by washing with dilute HCl and acetone, and then washed with distilled water before the measurements are taken.

2.2 Electrolyte

The corrosive electrolyte medium was prepared by dilution of analytical grade, H_2SO_4 (E. Merck). The concentration range of the synthesized Schiff's base used for the study is from 100 to 400 ppm. All solutions were prepared using double-distilled water.

2.3 Inhibitor

1,2,4-Triazole precursor, (4-amino-4H-1,2,4-triazole-3,5-diyl)dimethanol (ATD) is prepared by the condensation of glycolic acid with hydrazine hydrate. Hydrazine monohydrate (E. Merck) (0.75 mol) was added drop wise at 0 °C to 70% aqueous glycolic acid (E. Merck) (0.50 mol). The resulting solution was refluxed at 120 °C for 6 h. Then the reflux condenser was replaced with a downward condenser, and the reaction mixture was heated at 160 °C for a further 18 h allowing excess hydrazine hydrate and water to distil off. After cooling, the yellowish crystalline solid was obtained which is recrystallized from water to give analytically pure ATD [30]. The Schiff's base, HATD, was prepared by the condensation of ATD with 4-hydroxybenzaldehyde (E. Merck) (1:1 molar ratio) using alcohol as the solvent.

2.4 Weight Loss Measurements

The weight loss method is important in monitoring inhibition efficiency because of its simplicity and reliability. Experiments were carried out in a 250-ml beaker containing test solution under total immersion condition at 303 K. The pre-weighed mild steel samples of 1.8 × 2.1 cm^2 area were exposed to 0.5, 1, 1.5, and 2 N H_2SO_4 solutions in the absence and presence of different concentrations of HATD. After exposure, the specimens were washed initially under running tap water, to remove loosely adhering corrosion products and then cleaned with 15% HCl followed by acetone. From the weight loss in each measurement, the corrosion rate was calculated in milligram per centimeter square per hour (mg/cm^2 h). Experiments were repeated minimum four times to ascertain consistency. Whenever the variations are more than 1%, the data were confirmed by further repetition. The corrosion rate (C.R.), surface coverage (θ), and inhibition efficiency (%IE) were calculated using the following relation [31]:

$$\text{C.R} = \frac{W}{A \cdot t}, \tag{1}$$

where W is the weight loss (mg), A is the surface area (cm^2), and t is the time (h).

$$\theta = \frac{W_0 - W}{W_0}, \tag{2}$$

$$\%\text{IE} = \frac{W_0 - W}{W_0} \times 100, \tag{3}$$

where W_0 and W are the weight losses in uninhibited and inhibited solutions, respectively. Effects of inhibitor concentration and acid concentration on inhibition efficiency have been investigated by the weight loss measurements.

2.5 Electrochemical Studies

Electrochemical tests were carried out in a conventional three-electrode corrosion cell with platinum as the auxiliary electrode and saturated calomel electrode (SCE) as the reference electrode. The working electrode was first immersed in the test solution, and, after establishing a steady-state open-circuit potential (OCP), the electrochemical measurements were carried out in a Gill AC computer-controlled electrochemical workstation (ACM, UK, model no: 1475). The polarization curves were obtained in the potential range from −250 to +250 mV with respect to SCE at a sweep rate of 60 mV/min. The inhibition efficiency can be calculated from the corrosion current density as [32]

$$\text{IE}(\%) = \frac{i_{\text{corr}} - i^*_{\text{corr}}}{i_{\text{corr}}} \times 100, \tag{4}$$

where i_{corr} and i^*_{corr} represent the corrosion current density values without and with inhibitor, respectively. Similar experimental procedure is used for electrochemical impedance spectroscopy (EIS) technique. The studies were carried out at OCP in the frequency range of 0.1–10,000 Hz using 10 mV peak for peak voltage excitation. Inhibition efficiency is estimated using the following relation [33],

$$\mathrm{IE}(\%) = \frac{R^*_{ct} - R_{ct}}{R^*_{ct}} \times 100, \quad (5)$$

where R_{ct} and R^*_{ct} are the charge transfer resistance in the absence and presence of inhibitors, respectively. For electrochemical studies, 1 cm^2 area of the electrode was exposed in each experiment.

2.6 Surface Morphological Studies

Surface analysis was carried out to monitor the changes that occurred on mild steel surface due to corrosion process with and without the addition of inhibitor. Metal samples were immersed in 0.5 N H_2SO_4 solution for 3 h in the absence and presence of 400 ppm HATD. A preliminary analysis is carried out by a stereomicroscope (LeicaM80 model). To confirm the results obtained from microscopic technique, SEM images were taken by a scanning electron microscope model SU6600 (Serial No: HI-2102-0003) with an accelerating voltage of 12.0 kV at 250× magnification.

2.7 Computational Studies

Complete geometry optimization of the inhibitor molecule, HATD, was performed using density functional theory (DFT) with Becks three-parameter exchange functional along with Lee–Yang–Parr non-local correlation functional (B3LYP) with 6-31G* basis set using the Gaussian 03 programme package.

3 Results and Discussions

3.1 Weight Loss Analysis

The weight loss in the mild steel samples after exposure in corrosive electrolyte medium both in the absence and presence of HATD was examined. The values of corrosion rate and inhibition efficiency are listed in Table 1. From the table, it is clear that the corrosion rate of mild steel has been considerably decreased by the addition of HATD and there is a gradual decrease in corrosion rate by increasing the inhibitor concentration. Correspondingly, an increase in inhibition efficiency is observed with the concentration of inhibitor. When the inhibition performance was monitored in four different concentrations of H_2SO_4, it is observed that the corrosion rate of both in the absence and presence of inhibitor has been increased with the increase in acid concentration. However, the inhibitor HATD showed its best performance

Table 1 Data obtained from the weight loss analysis of mild steel samples in the absence and presence of HATD at different concentrations of H_2SO_4 solutions

Acid conc. (N)	$C_{inh.}$ (ppm)	C.R (mg/cm^2 h)	Surface cove. (θ)	η (%)
0.5	Blank	9.86	–	–
	100	4.26	0.568	56.8
	200	2.09	0.787	78.7
	300	1.08	0.889	88.9
	400	0.92	0.907	90.7
1.0	Blank	12.18	–	–
	100	6.88	0.435	43.5
	200	5.65	0.536	53.6
	300	4.31	0.646	64.6
	400	3.36	0.724	72.4
1.5	Blank	17.35	–	–
	100	11.04	0.363	36.3
	200	9.19	0.470	47.0
	300	7.85	0.548	54.8
	400	6.79	0.608	60.8
2	Blank	18.51	–	–
	100	16.04	0.133	13.3
	200	13.35	0.279	27.9
	300	10.73	0.419	41.9
	400	8.14	0.560	56.0

in 0.5 N H_2SO_4. Also it is noted that the inhibition efficiency decreases with increase in acid concentration.

3.2 Electrochemical Studies

Due to high inhibition efficiency of HATD in 0.5 N H_2SO_4, it is indented to study the electrochemical behavior and temperature response of mild steel corrosion in this concentration. Polarization measurements are commonly accepted to provide the relevant information about the kinetics of electrochemical corrosion parameters. Generally, the changes observed in the E_{corr} values of Tafel plots are used to classify inhibitors as anodic, cathodic, or mixed type. Cathodic and anodic polarization curves recorded for corrosion of mild steel in 0.5 N H_2SO_4 in the absence and presence of HATD at different temperatures are given in Fig. 1a–c. The addition of HATD caused a very small shift in E_{corr} value, indicating the mixed type behavior of the inhibitor [34–36]. Polarization parameters such as corrosion potential (E_{corr}), anodic and cathodic Tafel slopes (β_a and β_c), and corrosion current density (i_{corr}) are provided in Table 2. In acidic solutions, the anodic corrosion reaction is the dissolution of metal ions to corrosive medium and cathodic reaction is the evolution of hydrogen gas by the discharge of hydrogen ions. The addition of inhibitor may affect the anodic or cathodic, or both the reactions. Figure 1a–c reveals that the presence of HATD shifts both the anodic and cathodic curves to lower current densities (i_{corr}) which indicates the suppressed anodic metal dissolution and cathodic hydrogen evolution in the presence of HATD. Also with the increase in the concentration of inhibitor, i_{corr} value decreased and hence percentage inhibition efficiency has been increased as shown in Table 2. Almost parallel anodic and cathodic curves in the absence and presence of various concentrations of HATD suggest that the presence of inhibitor molecules prevents the mild steel corrosion through merely blocking the reaction sites on the surface without affecting the mechanism of cathodic hydrogen evolution reaction and anodic metal dissolution [37].

The modification of electrochemical process at metal/solution interface in the presence of inhibitors is better defined by Nyquist plots obtained from EIS analysis. EIS have proven to be a very useful and reliable method as it does not disturb the double layer at metal solution interface. Impedance parameters obtained for mild steel in 0.5 N H_2SO_4 in the absence and presence of different concentrations of HATD at temperatures 303, 308, and 313 K are presented in Table 3, and corresponding Nyquist plots are shown in Fig. 2a–c. As shown in Fig. 2a–c, the impedance loops do not yield perfect semicircles as expected from EIS theory and the deviation has been attributed to surface roughness and inhomogeneity of electrode surfaces [38, 39]. But it is clear from the plots that the impedance

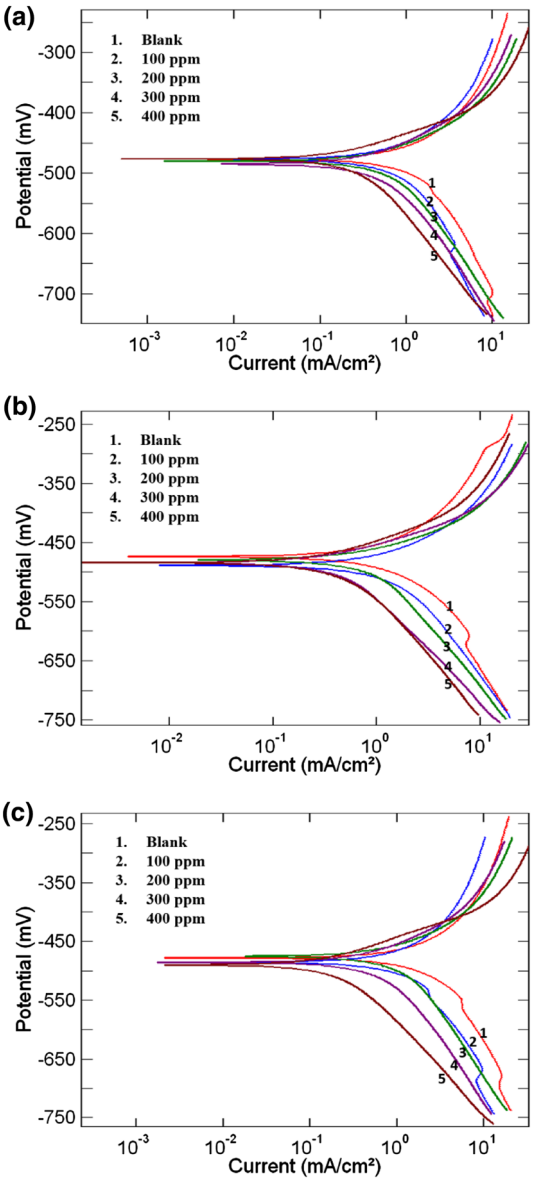

Fig. 1 Potentiodynamic polarization curves for mild steel in 0.5 N H_2SO_4 in the absence and presence of HATD at temperature **a** 303 K, **b** 308 K and **c** 313 K

response of mild steel in H_2SO_4 solution was significantly altered after the addition of inhibitor molecule. The diameter of capacitive loops increases with increase in inhibitor concentration which can be related to the increase in surface coverage of inhibitor on metal surface by adsorption process [40]. A slightly depressed single semicircle of Nyquist plots implies that corrosion of mild steel in 0.5 N H_2SO_4 solution is mainly controlled by a single charge transfer process [41–43]. The value of charge transfer resistance (R_{ct}) increases and corrosion current density (i_{corr}) decreases with increase in concentration of HATD which proves the formation of protective film on mild steel surface in the presence inhibitor.

Table 2 Potentiodynamic polarization parameters for mild steel in 0.5 N H_2SO_4 in the absence and presence of different concentrations of HATD

Temp. (K)	Conc. (ppm)	E_{corr} (mV)	βa (mV)	βc (mV)	i_{corr} (mA/cm^2)	C.R (mm/years)	C.R (mils/years)	IE%
303	Blank	−475	183	260	1.5640	18.126	713.65	
	100	−477	123	196	0.7801	9.0415	355.96	50.1
	200	−478	75.3	153	0.5168	5.9908	235.86	66.9
	300	−484	81.6	156	0.4209	4.8793	192.09	73.1
	400	−475	48.1	95.1	0.1465	1.6988	66.884	90.6
308	Blank	−488	225	239	2.0181	23.390	920.87	
	100	−490	106	160	1.1116	12.883	507.23	44.9
	200	−478	68.1	155	0.7151	8.2891	326.34	64.6
	300	−482	67.2	178	0.4583	5.3117	209.12	77.3
	400	−482	62.1	121	0.2898	3.3596	132.27	85.6
313	Blank	−478	233	271	3.0017	34.79	1369.6	
	100	−487	214	231	1.6715	19.372	762.70	44.4
	200	−474	112	236	1.3090	15.172	597.33	56.5
	300	−485	106	213	0.7939	9.2022	362.29	73.6
	400	−491	78.1	193	0.5144	5.9628	234.75	82.9

Table 3 Electrochemical impedance parameters for mild steel in 0.5 N H_2SO_4 in the absence and presence of different concentration of HATD

Temp. (K)	Conc. (ppm)	R_{ct} (Ω cm^2)	i_{corr} (mV/cm^2)	C.R (mm/years)	C.R (mils/years)	*E%*
303	Blank	7.241	3.6030	41.75	1644	
	100	15.92	1.6390	18.99	747.7	54.5
	200	22.42	1.1640	13.49	530.9	67.7
	300	32.32	0.8071	9.355	368.3	77.6
	400	69.30	0.3764	4.363	171.8	89.6
308	Blank	5.193	5.0230	58.22	2292	
	100	9.515	2.7420	31.78	1251	45.4
	200	15.07	1.7310	20.06	789.9	65.5
	300	28.56	0.9134	10.59	416.8	81.8
	400	38.66	0.6748	7.821	307.9	86.6
313	Blank	4.649	5.6110	65.04	2560	
	100	8.529	3.0591	35.45	1396	45.4
	200	11.48	2.2721	26.34	1037	59.5
	300	16.32	1.5980	18.53	729.4	71.5
	400	22.73	1.1480	13.30	523.7	79.5

3.3 Effect of Temperature

To evaluate the effect of temperature on inhibition efficiency, polarization and impedance studies were carried out at three different temperatures (303,308 and 313 K) and corresponding plots are shown in Figs. 1a–c and 2a–c. The inhibition efficiency values calculated from the evaluation of Tafel and Nyquist plots are listed in Tables 2 and 3, respectively. A comparison of inhibition efficiency values obtained at different temperatures is graphically represented in Fig. 3. The figure reveals that inhibition efficiency decreases with increase in temperature. The decrease in inhibition efficiency with increase in temperature is attributed to desorption of inhibitor molecules from metal which in turn increases the surface area available for corrosive environment to contact with metal [44]. The effect of temperature on corrosion rate can be represented by Arrhenius equation as [45],

$$\log(\text{C.R.}) = \log A - \frac{E_a}{2.303RT}, \quad (6)$$

where E_a is the apparent activation energy, T is the absolute temperature, A is the Arrhenius pre-exponential constant, and R is the gas constant. Figure 4 shows linear plots of log (C.R.) against $1/T$ for mild steel in 0.5 N H_2SO_4, which indicates that corrosion process follows the Arrhenius

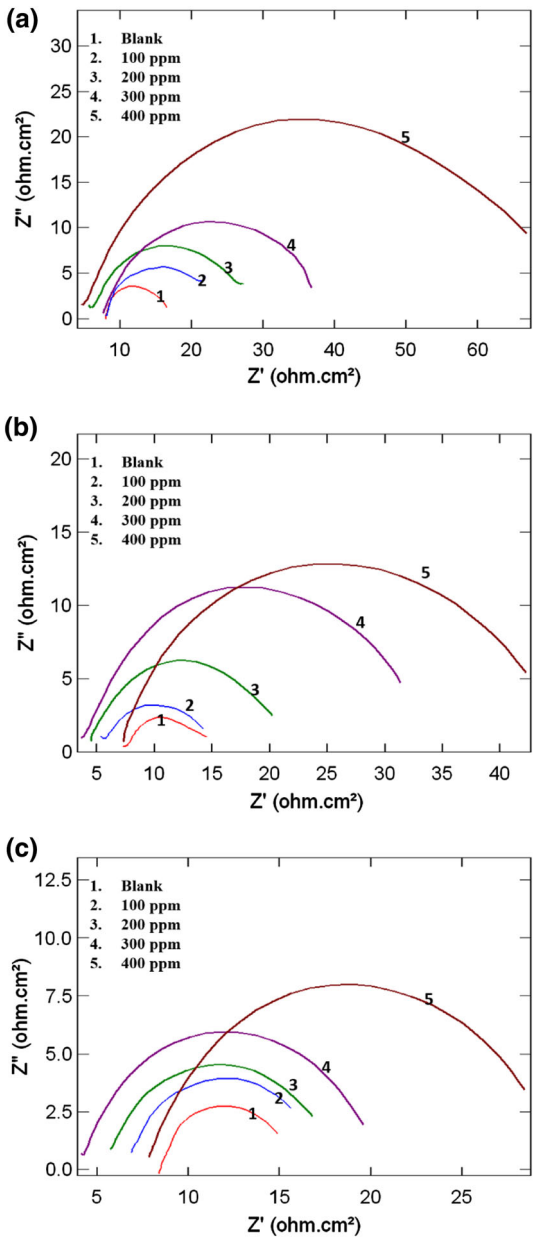

Fig. 2 Nyquist plot for mild steel for mild steel in 0.5 N H_2SO_4 in the absence and presence of HATD at temperature **a** 303 K, **b** 308 K and **c** 313 K

equation. The values of activation energy E_a calculated from the slope of Arrhenius plot are given in Table 4. It is seen that the value of E_a for inhibited solution is greater than that for uninhibited solution and it increases with the increase in concentration of inhibitor. The increased value of E_a in inhibited solution indicates the formation of high-energy barrier against the corrosion process due to the formation of adsorbed film on mild steel surface. The adsorbed film protects mild steel from acid attack by preventing charge/mass transfer reaction occurring on the surface [46–49]. Other kinetic parameters such as enthalpy of adsorption (ΔH) and entropy of adsorption (ΔS) were obtained from transition state equation

$$\text{C.R.} = \frac{RT}{Nh} e^{\left(\frac{\nabla S}{R}\right)} e^{\left(\frac{-\nabla H}{RT}\right)}, \tag{7}$$

where N is the Avogadro number, h is the Planck's constant, R is the universal gas constant, and T is the absolute temperature. As shown in Fig. 5, the plot of log (C.R./T) against (1/T) in the absence and presence of HATD gave straight line, where the slope represents ($-\Delta H/2.303R$) and intercept represents ($\log(R/Nh) + \Delta S/2.303R$). The enthalpy and entropy of activation calculated from slope and intercepts are presented in Table 4. The positive sign of ΔH both in the absence and presence of inhibitor indicates the endothermic nature of mild steel dissolution in test solution. Again, the value of ΔH increases with increase in inhibitor concentration since dissolution process becomes more difficult by increasing inhibitor concentration. The values of entropy of activation in the presence of inhibitor are less negative when compared to blank solution which suggests an increase in randomness during the formation of activated complex [50, 51].

3.4 Adsorption Isotherm

The inhibition mechanism follows adsorption of inhibitors on metal surface, and extend of inhibition is related to degree of surface coverage. An adsorption isotherm defines the relation of concentration of inhibitor to surface area covered and provides significant information whether the mode of adsorption is physisorption or chemisorption. Among various isotherms, Langmuir adsorption isotherm was found to be the best fit for inhibition of HATD on mild steel in 0.5 N H_2SO_4. The fractional surface coverage θ, at different concentrations of HATD in 0.5 N H_2SO_4 solution, was determined from corresponding impedance data as follows:

$$\theta = \frac{R_{ct}^{*} - R_{ct}}{R_{ct}^{*}}. \tag{8}$$

According to Langmuir adsorption isotherm, the surface coverage (θ) is related to concentration of inhibitor (C) by the equation

$$\frac{\theta}{1-\theta} = KC. \tag{9}$$

On rearranging,

$$\frac{C}{\theta} = \frac{1}{K} + C, \tag{10}$$

where K is the equilibrium constant for adsorption process, plot of C/θ as function of C gave a straight line as shown in Fig. 6 from which equilibrium constant is obtained as the

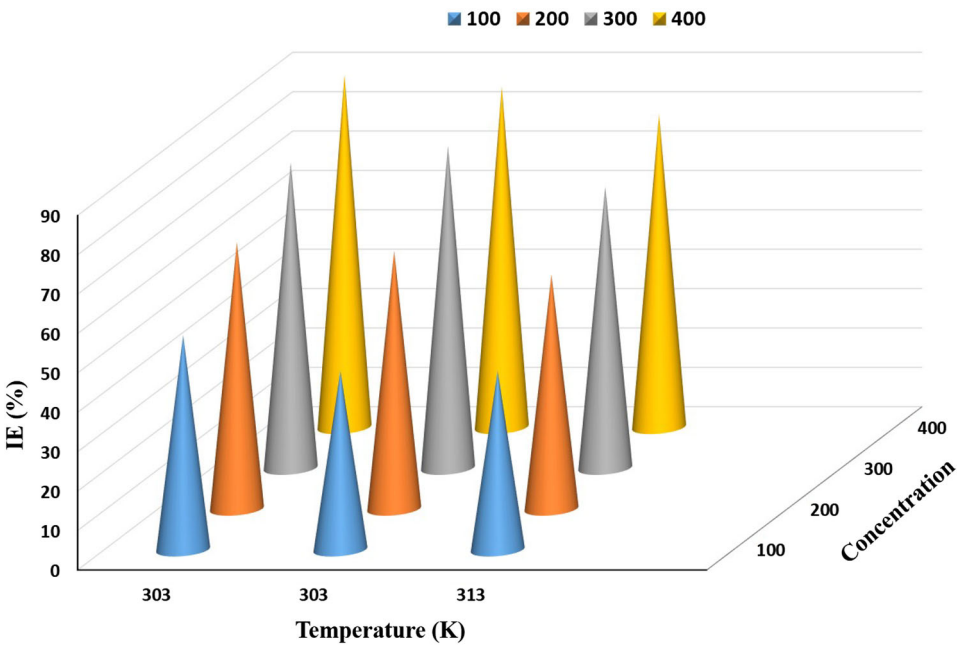

Fig. 3 Effect of temperature and concentration of HATD on inhibition efficiency for corrosion of mild steel in 0.5 N H_2SO_4 solution

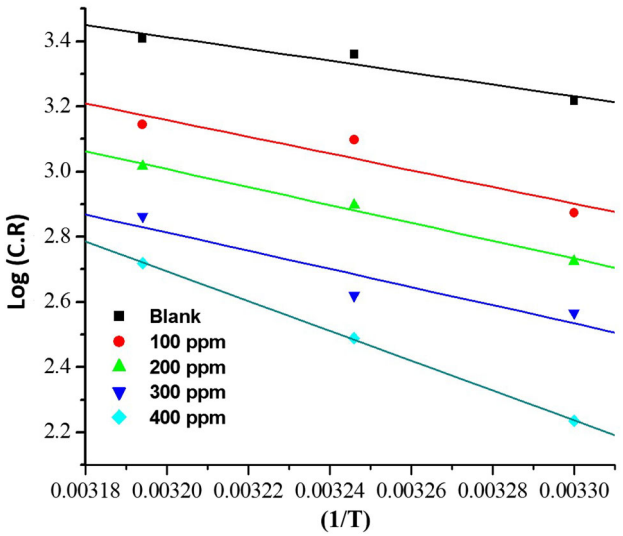

Fig. 4 Arrhenius plot of log (C.R) against (1/*T*) for mild steel corrosion in 0.5 N H_2SO_4 solution in the absence and presence of HATD

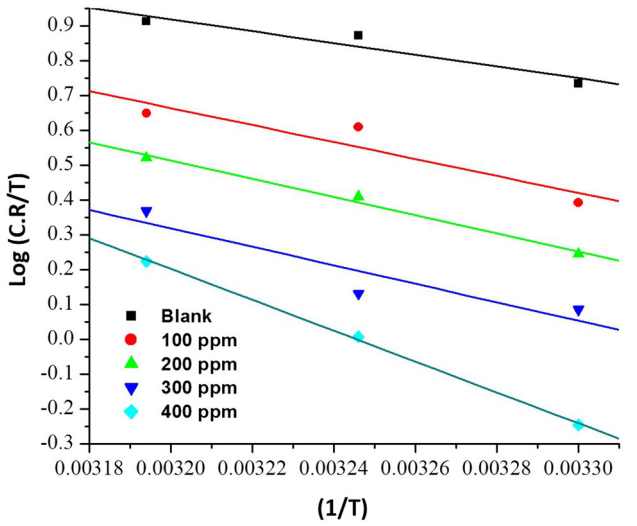

Fig. 5 Plot of log (C.R/*T*) against (1/*T*) for mild steel in 0.5 N H_2SO_4 solution in the absence and presence of HATD

Table 4 Thermodynamic activation parameters for mild steel in 0.5 N H_2SO_4 solution at different concentrations of inhibitor

Conc. (ppm)	E_a (kJ/mol)	ΔH (kJ/mol)	ΔS (J/mol k)
Blank	34.87	32.29	−77.05
100	49.16	46.62	−36.03
200	52.57	50.03	−28.03
300	53.36	50.83	−29.17
400	87.42	84.89	77.60

reciprocal of intercept. The values of standard free energy of adsorption ΔG is associated to K by the relation

$$\Delta G = -2.303RT\log(55.5K), \tag{11}$$

where R is the universal gas constant, T is the absolute temperature, and 55.5 refers to concentration of water in solution represented in M. If the value of ΔG is in the order of −20 kJ/mol or lower, the mechanism follows physisorption, and if it is in order of −40 kJ/mol or higher the mechanism follows chemisorption [52]. From data presented in Table 5, it can be concluded that the adsorption of HATD on mild steel in 0.5 N H_2SO_4 involves both chemisorption and physisorption.

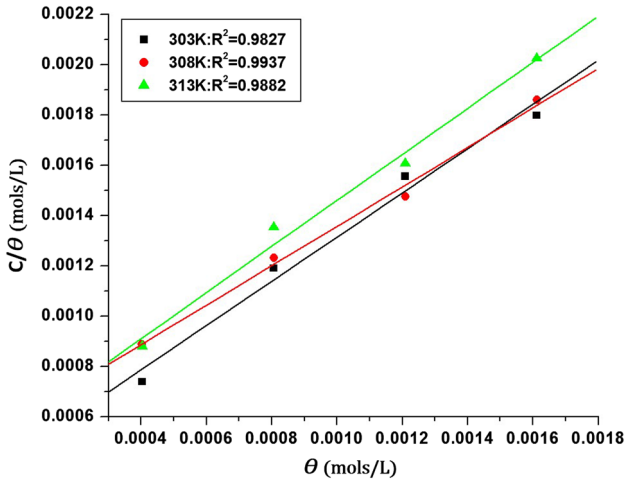

Fig. 6 Langmuir adsorption isotherm for mild steel corrosion in 0.5 N H_2SO_4 solution containing HATD at different temperatures

Table 5 The values of equilibrium constant (K) and standard free energy change (ΔG) for mild steel in 0.5 N H_2SO_4 solution at different temperatures

Temp. (K)	Equilibrium constant (mol^{-1})	Free energy change (kJ/mol)
303	2296.5	29.62
308	1744.4	29.40
313	1836.2	30.01

3.5 Surface Morphological Studies

Surface morphologies of mild steel in 0.5 N H_2SO_4 in the absence and presence of HATD obtained by stereomicroscopic technique and SEM are shown in Figs. 7a–c and 8a–c, respectively. From the surface images, it is clear that mild steel is highly corroded in 0.5 N H_2SO_4 in the absence of HATD. When inhibitor is added to the test solution, the surface of mild steel shows close resemblance to bare mild steel surface. This observation evidently reveals that HATD decreases the corrosion of mild steel by forming a good molecular film on the surface and prevents the interaction between mild steel surface and aggressive solution to a greater extent.

3.6 Quantum Chemical Studies

Quantum chemical parameters such as energy of highest occupied molecular orbital (E_{HOMO}), lowest unoccupied molecular orbital (E_{LUMO}), energy gap (ΔE), and dipole moment were calculated, and are given in Table 6. The optimized geometry, HOMO, and LUMO are presented in Fig. 9a–c. The inhibition property can be discussed on the basis of donor–acceptor interaction between metal and inhibitor since the corrosion involves adsorption mechanism. According to Frontier molecular orbital theory, E_{HOMO} is associated with electron donating ability and E_{LUMO} is associated with electron accepting ability of molecule [53]. From Fig. 9a–c, it is clear that both triazole and benzylidene rings contribute significantly to the HOMO, which shows the tendency of molecule to donate charges to vacant orbitals of metal atom. However, the contribution to LUMO is mainly from benzylidene ring, which can be attributed to electron withdrawing effect of benzene ring in retro-donation step. Again, a low value of energy gap (ΔE) is an indication of high reactivity of inhibitor molecule.

3.7 Mechanism of Corrosion Inhibition

A general mechanism proposed for the dissolution of metal and hydrogen evolution when mild steel exposed in H_2SO_4 in the absence of inhibitor is [53],

Anodic metal dissolution:

$$Fe + SO_4^{2-} \rightleftharpoons (FeSO_4^{2-})_{ads}, \quad (12)$$

$$(FeSO_4^{2-})_{ads} \rightleftharpoons (FeSO_4)_{ads} + 2e, \quad (13)$$

$$(FeSO_4)_{ads} \rightleftharpoons Fe^{2+} + SO_4^{2-}. \quad (14)$$

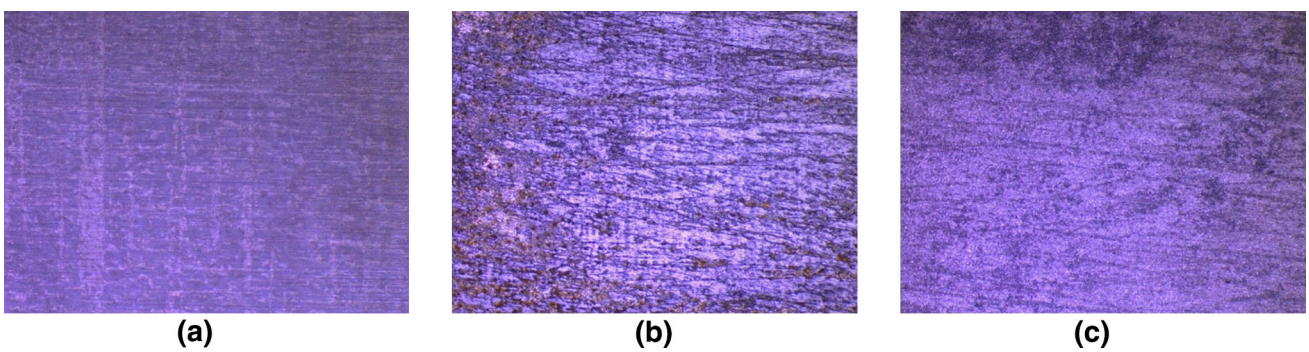

Fig. 7 Optical images of mild steel specimen **a** bare mild steel, **b** mild steel in 0.5 N H_2SO_4 solution, and **c** mild steel in 0.5 N H_2SO_4 solution in the presence of 400 ppm HATD

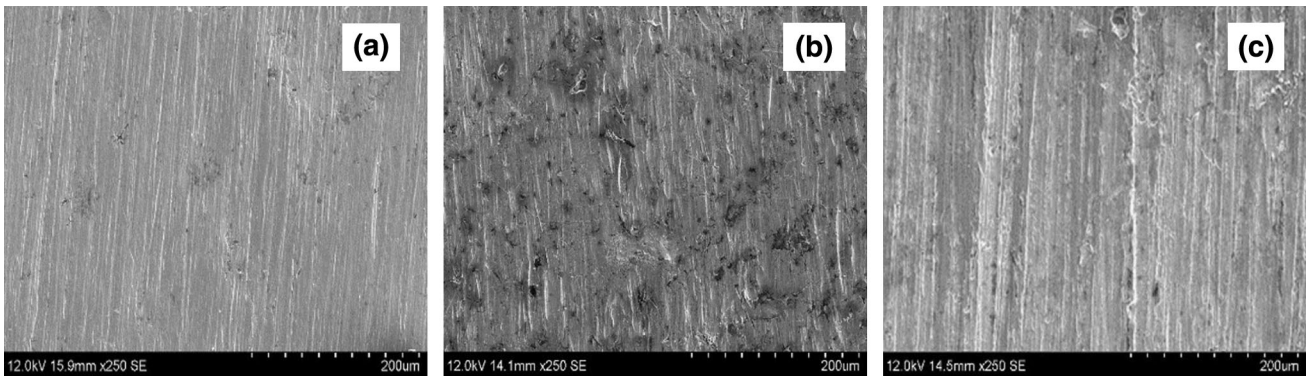

Fig. 8 SEM images of mild steel specimen **a** bare mild steel, **b** mild steel in 0.5 N H_2SO_4 solution, and **c** mild steel in 0.5 N H_2SO_4 solution in the presence of 400 ppm HATD

Table 6 Electronic parameters of HATD obtained from quantum mechanical studies

Total energy (eV)	E_{HOMO} (eV)	E_{LUMO} (eV)	ΔE (eV)	Dipole moment (D)
−23700	−6.490062	−1.7396	4.7504	5.5218

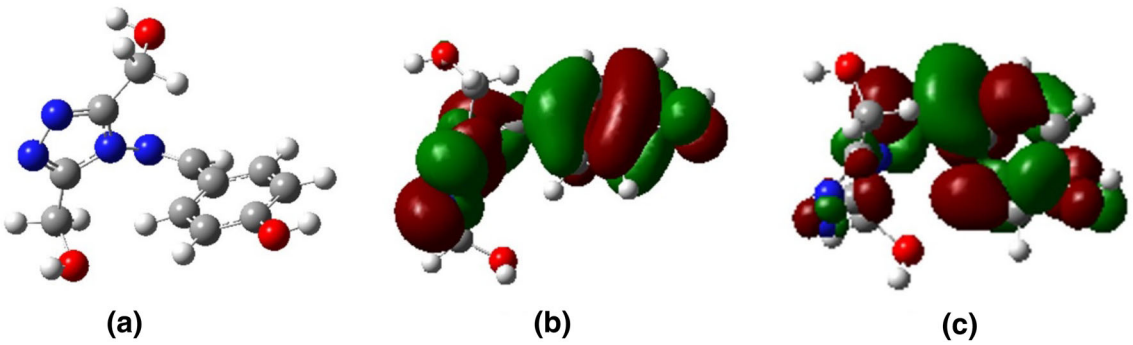

Fig. 9 Images of **a** optimized geometry, **b** HOMO, and **c** LUMO of the inhibitor HATD

Cathodic hydrogen evolution:

$$Fe + H^+ \rightleftharpoons (FeH^+)_{ads}, \quad (15)$$

$$(FeH^+)_{ads} + e \rightleftharpoons (FeH)_{ads}, \quad (16)$$

$$(FeH)_{ads} + H^+ + e \rightleftharpoons Fe + H_2. \quad (17)$$

In the presence of inhibitors, the first stage in the mechanism of inhibition is the adsorption of molecules on the metal surface by the replacement of water molecules. The adsorption phenomenon of organic molecules generally involves physisorption, chemisorption, or a combination of both. The standard free energy values given in Table 5 indicate that the adsorption of HATD on mild steel surface in 0.5 N H_2SO_4 solution involves both physisorption and chemisorption. Physisorption requires the presence of an electrically charged surface and charged species in the bulk of the solution. Since the HATD molecule contains π electrons and N and O atoms with lone pair of electrons, it can be easily protonated in H_2SO_4 solution. The electrostatic interaction takes place between the protonated inhibitor molecule ($HATDH^+$) and $(FeSO_4)^{2-}_{ads}$ species on mild steel surface as follows:

$$(FeSO_4^{2-})_{ads} + (HATDH^+) \rightleftharpoons (FeSO_4^{2-}(HATDH^+))_{ads}. \quad (18)$$

The above process causes a retardation in the metal dissolution reaction. The protonated inhibitor molecules may also be adsorbed at cathodic reaction sites in competition with hydrogen ions, thereby reducing the rate of hydrogen evolution. The chemical adsorption arises from the donor–acceptor interactions between lone pair of electrons or π electrons of the inhibitor molecule and vacant d orbitals of Fe atoms of mild steel surface.

4 Conclusions

The synthesized 1,2,4- triazole Schiff's base, HATD, showed good inhibition efficiency towards mild steel in H_2SO_4. The inhibition efficiency measured through

potentiodynamic polarization and electrochemical impedance studies are in good agreement. Potentiodynamic polarization studies revealed the mixed type behavior of the inhibitor. The inhibition efficiency increased with increase in inhibitor concentration and decreased with acid concentration and temperature. The inhibition action of HATD proceeds through adsorption, which obeys Langmuir adsorption isotherm. The positive sign of ΔH indicates endothermic nature of corrosion process. Basic computational calculations revealed the optimized geometry of the inhibitor molecule.

References

1. Zakaria K, Negm NA, Khamis EA, Badr EA (2016) Electrochemical and quantum chemical studies on carbon steel corrosion protection in 1 M H_2SO_4 using new eco-friendly Schiff base metal complexes. J Taiwan Inst Chem Eng 61:316–326
2. Fouda SAS, Mahmoud WM, Mageed HAA (2016) Evaluation of an expired nontoxic amlodipine besylate drug as a corrosion inhibitor for low-carbon steel in hydrochloric acid solutions. J Bio Tribo Corros 2:7
3. Tezeghdenti M, Dhouibi L, Etteyeb N (2015) Corrosion inhibition of carbon steel in 1 M sulphuric acid solution by extract of eucalyptus globulus leaves cultivated in Tunisia arid zones. J Bio Tribo Corros 1:16
4. Mohsenifar F, Jafari H, Sayin K (2016) Investigation of thermodynamic parameters for steel corrosion in acidic solution in the presence of *N*,*N*1-Bis(phloroacetophenone)-1,2-propanediamine. J Bio Tribo Corros 2:1
5. Ebrahimzadeh M, Gholamia M, Momenia M, Kosari A, Moayeda MH, Davood A (2015) Theoretical and experimental investigations on corrosion control of 65Cu–35Zn brass in nitric acid by two thiophenol derivatives. Appl Surf Sci 332:384–392
6. Paul S, Koley I (2016) Corrosion inhibition of carbon steel in acidic environment by papaya seed as green inhibitor. J Bio Tribo Corros 2:6
7. Mourya P, Banerjee S, Rastogi RB, Singh MM (2013) Inhibition of mild steel corrosion in hydrochloric and sulfuric acid media using a thiosemicarbazone derivative. Ind Eng Chem Res 52:12733–12747
8. Yadav M, Kumar S, Bahadur I, Ramjugernath D (2014) Corrosion inhibition effect of synthesized thiourea derivatives on mild steel in a 15% HCl solution. Int J Electrochem Sci 9:6529–6550
9. Sasikumar Y, Adekunle AS, Olasunkanmi LO, Bahadur I, Baskar R, Kabanda MM, Obot IB, Ebenso EE (2015) Experimental, quantum chemical and Monte Carlo simulation studies on the corrosion inhibition of some alkylimidazolium ionic liquids containing tetrafluoroborate anion on mild steel in acidic medium. J Mol Liq 211:105–118
10. Fouda AS, Megahed HE, Fouad N, Elbahrawi NM (2016) Corrosion inhibition of carbon steel in 1 M hydrochloric acid solution by aqueous extract of thevetia peruviana. J Bio Tribo Corros 2:16
11. Vashisht H, Kumar S, Bahadur I, Singh G (2013) Evaluation of (2-hydroxyethyl)triphenylphosphonium bromide as corrosion inhibitor for mild steel insulphuric acid. Int J Electrochem Sci 8:684–699
12. Mourya P, Singh P, Rastogi RB, Singh MM (2016) Inhibition of mild steel corrosion by 1,4,6-trimethyl-2-oxo-1,2-dihydropyridine-3-carbonitrile and synergistic effect of halide ion in 0.5 M H_2SO_4. Appl Surf Sci 380:141–150
13. Ansari KR, Quraishi MA, Singh A (2014) Schiff's base of pyridyl substituted triazoles as new and effective corrosion inhibitors for mild steel in hydrochloric acid solution. Corros Sci 79:5–15
14. Yuan C, Liu X, Wu Y, Lu L, Zhu M (2016) A triazole Schiff base-based selective and sensitive fluorescent probe for Zn^{2+}: a combined experimental and theoretical study. Spectrochim Acta Part A Mol Biomol Spectrosc 154:215–219
15. Tourabi M, Nohair K, Nyassi A, Hammouti B, Jama C, Bentiss F (2014) Thermodynamic characterization of metal dissolution and inhibitor adsorption processes in mild steel/3,5-bis(3,4-dimethoxyphenyl)-4-amino-1,2,4-triazole/hydrochloric acid system. J Mater Environ Sci 5(4):1133–1143
16. ElBelghiti M, Karzazi Y, Dafali A, Hammouti B, Bentiss F, Obot IB, Bahadur I, Ebenso EE (2016) Experimental, quantum chemical and Monte Carlo simulation studies of 3,5-disubstituted-4-amino-1,2,4-triazoles as corrosion inhibitors on mild steel in acidic medium. J Mol Liq 218:281–293
17. Yadav M, Kumar S, Sinha RR, Bahadur I, Ebenso EE (2015) New pyrimidine derivatives as efficient organic inhibitors on mild steel corrosion in acidic medium: electrochemical, SEM, EDX, AFM and DFT studies. J Mol Liq 211:135–145
18. Joseph B, Prajila M, Joseph A (2012) Inhibition of mild steel corrosion in 1 M hydrochloric acid using (E)-(4-(4-methoxybenzylideneamino)-4H-1,2,4-triazole-3,5-diyl)dimethanol (MBATD). J Dispersion Sci Technol 33:739–749
19. Ramya K, Joseph A (2015) Dependence of temperature on the corrosion protection properties of vanillin and its derivative, HMATD, towards copper in nitric acid: theoretical and electroanalytical studies. Res Chem Intermed 41:1053–1077
20. Guo L, Zhu S, Zhang S, He Q, Li W (2014) Theoretical studies of three triazole derivatives as corrosion inhibitors for mild steel in acidic medium. Corros Sci 87:366–375
21. Kuruvilla M, John S, Joseph A (2016) Electroanalytical studies on the interaction of L-serine-based Schiff base, HHDMP, with copper in sulphuric acid. J Bio Tribo Corros 2:19
22. Shabbir M, Akhter Z, Ahmad I, Ahmed S, Ismail H, Mirza B, McKee V, Bolte M (2016) Synthesis, characterization, biological and electrochemical evaluation of novel ether based ON donor bidentate Schiff bases. J Mol Liq 1116:84–92
23. Ghosh P, Kumarb N, Mukhopadhyayc SK, Banerjeea P (2016) Sensitive and fluorescent Schiff base chemo sensor for Pico molar level fluoride detection: in vitro study and mimic of logic gate function. Sens Actuator B Chem 224:899–906
24. Marwani HM, Asiri AM, Khan SA (2014) Spectrophotometric and spectrofluorometric studies of novel heterocyclic Schiff base dyes. King Saud Univ Arab J Chem 7:609–614
25. Asiri AM, Khan SA, Marwani HM, Sharma K (2013) Synthesis, spectroscopic and physicochemical investigations of environmentally benign heterocyclic Schiff bases derivatives as antibacterial agents on the bases of in vitro and density functional theory. J Photochem Photobiol B Biol 120:82–89
26. Nassar AAM, Hassan AM, Shoeib MA, El Kmash AN (2015) Synthesis, characterization and anticorrosion studies of new homobimetallic Co(II), Ni(II), Cu(II), and Zn(II) Schiff base complexes. J Bio Tribo Corros 1:19
27. Sılku P, Ozkınalı S, Ozturk Z, Asan A, Kose DA (2016) Synthesis of novel Schiff Bases containing acryloyl moiety and the investigation of spectroscopic and electrochemical properties. J Mol Struct 1116:72–83
28. Gupta NK, Verma C, Quraishi MA, AK M (2016) Schiff's bases derived from L-lysine and aromatic aldehydes as green corrosion inhibitors for mild steel: experimental and theoretical studies. J Mol Liq 215:47–57
29. Kumar CBP, Mohana KN (2014) Corrosion inhibition efficiency and adsorption characteristics of some Schiff bases at mild steel/hydrochloric acid interface. J Taiwan Inst Chem Eng 45(3):1031–1042

30. John S, Joy J, Prajila M, Joseph A (2011) Electrochemical, quantum chemical, and molecular dynamics studies on the interaction of 4-amino-4H,3,5-di(methoxy)-1,2,4-triazole (ATD), BATD, and DBATD on copper metal in 1 N H2SO4. Mater Corros 62:1031–1041
31. Anupama KK, Shainy KM, Joseph A (2016) Excellent anticorrosion behavior of Ruta Graveolens extract (RGE) for mild steel in hydrochloric acid: electro analytical studies on the effect of time, temperature, and inhibitor concentration. J Bio Tribo Corros 2:2
32. Anupama KK, Ramya K, Joseph A (2016) Electrochemical and computational aspects of surface interaction and corrosion inhibition of mild steel in hydrochloric acid by *Phyllanthus amarus* leaf extract (PAE). J Mol Liq 216:146–155
33. Ramya K, Joseph A (2015) Synergistic effects and hydrogen bonded interaction of alkyl benzimidazoles and thiourea pair on mild steel in hydrochloric acid. J Taiwan Inst Chem Eng 52:127–139
34. Daoud D, Douadi T, Hamani H, Chafaa S, Al Noaimi M (2015) Corrosion inhibition of mild steel by two new heterocyclic compounds in 1 M HCl: experimental and computational study. Corros Sci 94:21–37
35. Kuruvilla M, Prasad AR, John S, Joseph A (2017) Enhanced inhibition of the corrosion of metallic copper exposed in sulphuric acid through the synergistic interaction of cysteine and alanine: electrochemical and computational studies. J Bio Tribo Corros 3:5
36. Singh P, Singh A, Quraishi MA (2016) Thiopyrimidine derivatives as new and effective corrosion inhibitors for mild steel in hydrochloric acid: electrochemical and quantum chemical studies. J Taiwan Inst Chem Eng 60:588–601
37. Baran E, Cakir A, Yazici B (2016) Inhibitory effect of *Gentiana olivieri* extracts on the corrosion of mild steel in 0.5 M HCl: electrochemical and phytochemical evaluation. Arab J Chem. doi:10.1016/j.arabjc.2016.06.008
38. Elhadi SM, Bilel M, Abdelmalek B, Aissa C (2016) Experimental evaluation of quinolinium and isoquinolinium derivatives as corrosion inhibitors of mild steel in 0.5 M H_2SO_4 solution. Prot Met Phys Chem Surf 52:731–736
39. Shihab MS, Nazari MH, Fay L (2016) Study of inhibition effect of pyridinium salt derivative on corrosion of C1010 carbon steel in saline solution. Prot Met Phys Chem Surf 52:714–720
40. Mohan R, Anupama KK, Joseph A (2017) Effect of methyl, ethyl, and propyl substitution on benzimidazole for the protection of copper metal in nitric acid: theoretical and electrochemical screening studies. J Bio Tribo Corros 3:2
41. Ramya K, Mohan R, Joseph A (2014) Adsorption and electrochemical studies on the synergistic interaction of alkyl benzimidazoles and ethylene thiourea pair on mild steel in hydrochloric acid. J Taiwan Inst Chem Eng 45:3021–3032
42. Fouda AS, Sh Mohamed F, El-Sherbeni MW (2016) Corrosion inhibition of aluminum–silicon alloy in hydrochloric acid solutions using carbamidicthioanhydride derivatives. J Bio Tribo Corros 2:11
43. El-Abbasy HM, Nazeer AA, Fouda AS (2016) Electrochemical assessment of inhibitive behavior of some antibacterial drugs on 316 stainless steel in acidic medium. Prot Met Phys Chem Surf 52:562–573
44. Singh P, Quraishi MA (2016) Corrosion inhibition of mild steel using novel bis Schiff's bases as corrosion inhibitors: electrochemical and Surface measurement. Measurement 86:114–124
45. Ali Gurten A, Keles H, Bayol E, Kandemirli F (2015) The effect of temperature and concentration on the inhibition of acid corrosion of carbon steel by newly synthesized Schiff base. J Ind Eng Chem 27:68–78
46. Yesudass S, Olasunkanmi LO, Bahadur I, Kabanda MM, Obot IB, Ebenso EE (2016) Experimental and theoretical studies on some selected ionic liquids with different cations/anions as corrosion inhibitors for mild steel in acidic medium. J Taiwan Inst Chem Eng 64:252–268
47. Kairi NI, Kassim J (2013) The effect of temperature on the corrosion inhibition of mild steel in 1 M HCl solution by curcuma longa extract. Int J Electrochem Sci 8:7138–7155
48. Faustin M, Maciuk A, Salvin P, Roos C, Lebrini M (2015) Corrosion inhibition of C38 steel by alkaloids extract of *Geissospermum laeve* in 1 M hydrochloric acid: electrochemical and phytochemical studies. Corros Sci 92:287–300
49. Karimi A, Danaee I, Eskandari H, RashvanAvei M (2015) Electrochemical Investigations on the inhibition behavior and adsorption isotherm of synthesized di-(resacetophenone)-1,2-cyclohexandiimine Schiff base on the corrosion of steel in 1 M HCl. Prot Met Phys Chem Surf 51:899–907
50. Guan NM, Xueming L, Fei L (2004) Synergistic inhibition between *o*-ophenanthroline and chloride ion on cold rolled steel corrosion in phosphoric acid. Mater Chem Phys 86:59–68
51. Sudheer, Quraishi MA (2013) Electrochemical and theoretical investigation of triazole derivatives on corrosion inhibition behavior of copper in hydrochloric acid medium. Corros Sci 70:161–169
52. Verma C, Olasunkanmi LO, Obot IB, Ebenso EE, Quraishi MA (2016) 2, 4-Diamino-5-(phenylthio)-5H-chromeno [2,3-b] pyridine-3-carbonitriles as green and effective corrosion inhibitors: gravimetric, electrochemical, surface morphology and theoretical studies. RSC Adv 6:53933–53948
53. Doner A, Solmaz R, Ozcan M, Kardas G (2011) Experimental and theoretical studies of thiazoles as corrosion inhibitors for mild steel in sulphuric acid solution. Corros Sci 53:2902–2913